Bulk vortex matter in $Bi_2Sr_2CaCu_2O_{8+\delta}$ using Corbinol disk contacts

Y. M. Wang,* M. S. Fuhrer,† and A. Zettl
[1]*Department of Physics, University of California at Berkeley, and Materials Sciences Division, Lawrence Berkeley National Laboratory, Berkeley, California 94720, USA*

S. Nagashima, K. Oka, and Y. Nishihara
[2]*National Institute of Advanced Industrial Science and Technology, Tsukuba, Ibaraki 305, Japan*
(Received 20 September 2004; revised manuscript received 18 January 2005; published 22 April 2005)

We have studied bulk vortex properties in $Bi_2Sr_2CaCu_2O_{8+\delta}$ (BSCCO) using transport measurements with a unique Corbino disk contact geometry. This Corbino disk contact geometry allows us to measure true bulk vortex properties free from surface barrier effects. The investigated vortex properties include current-induced vortex dissipation in the vortex liquid and vortex solid phases, vortex matter phase transition (vortex lattice melting transition), and vortex correlation along the *c* axis of BSCCO. No discrepancy is found between our measurements and others measurements using the conventional four-probe contact geometry, which renders vortex transport properties susceptible to the Bean-Livingston surface barrier effect. We conclude that the sample bulk vortex matter properties determine the vortex transport behaviors in BSCCO.

DOI: 10.1103/PhysRevB.71.132507 PACS number(s): 74.25.Qt, 74.25.Sv, 74.25.Op

To study vortex behaviors in the highly anisotropic high-temperature superconductor $Bi_2Sr_2CaCu_2O_{8+\delta}$ (BSCCO) using transport measurement method, one needs to use four-probe contacts for the purpose of avoiding contact resistance. Among various four-probe contact geometries, Corbino-disk geometry has been the replacement for the widely used conventional four-point contact geometry, ever since the observation that the four-point contacts are vulnerable to the Bean-Livingston (BL) surface barrier effect.[1]

A set of Corbino-disk four-probe contacts consists of an outer ring enclosing a center contact for current injection, and two points in between the current contacts for voltage measurements. A set of conventional four-point contacts (conventional four-probe contacts) consists of four contact points (dots or horizontal bars) arranged in a row, with the end two contacts applying current and the center two contacts measuring the voltage. The exclusive advantage of the Corbino-disk contacts is that the current-driven transversely-moving vortices are confined inside the disk, and need not cross a surface boundary. As a result, the BL surface barrier effect, which comes into play when vortices cross the sample edges (as occurs when using the conventional four-probe contacts), is avoided. Although there have been a number of studies on vortex matter in BSCCO using the Corbino-disk contact geometry,[2–6] there remains a controversy in regard to whether it is the BL surface barrier sample edge effect on vortex or the samples own bulk vortex properties, such as pinning, that determines the observed vortex transport behavior in BSCCO.[4,5] To resolve this issue, we performed sensitive transport measurements using Corbino-disk contacts and probed true bulk vortex properties in BSCCO.

We have studied the bulk vortex lattice melting phase transition, the current-induced bulk vortex dissipation in both the vortex solid and the vortex liquid phases, and the bulk vortex correlation along the *c* axis of BSCCO using both the plain Corbino-disk contact geometry and a novel Corbino-disk flux-transformer contact geometry. All our observations via the Corbino-disk method are identical to those studied using the conventional four-probe geometry where vortex properties were believed to be determined by the BL surface barrier effect.[1] We therefore conclude that it is the samples own bulk vortex properties that determines the vortex transport properties in BSCCO, instead of the BL surface barrier effect.

Single crystals of BSCCO were grown using the floating zone method.[7] The sample measured in this experiment has a dimension of $1.2\ \text{mm} \times 1.3\ \text{mm} \times 20\ \mu\text{m}$. Gold Corbino-disk contacts were fabricated onto the sample using photolithography techniques. Figure 1 shows the schematic of the contacts. The Corbino disk measures 1 mm in diameter. Current travels from the center contact pad to the outer ring. Since the direction of the moving vortices is perpendicular to the direction of the driving current, vortices circulate within the disk and thus avoid crossing the sample edges. There are two pairs of voltage contacts: V_1 is a pair of surface voltage contacts and V_2 is a pair of hole voltage contacts etched to

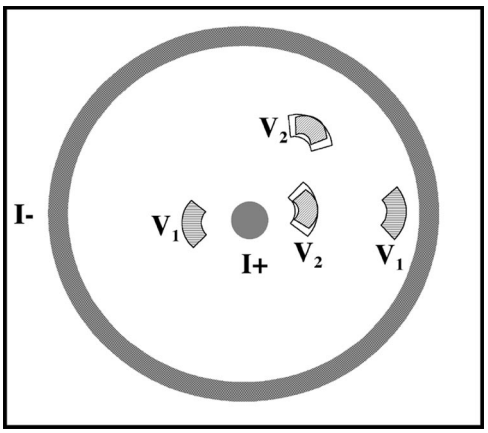

FIG. 1. Schematic of the Corbino-disk contacts on BSCCO patterned using photolithography. Surface contacts are denoted by V_1 and hole contacts are denoted by V_2. V_2 contacts are at 3 μm below the sample surface.

3 μm below the sample surface. The outer boxes of V_2 are the edges of the etched pattern and the shaded regions are the actual gold contact pads within. The two current contacts paired with V_1 comprise the standard Corvino-disk contact; while the two current contacts paired with V_2 form an unconventional Corbino-disk geometry, which we term the Corbino-disk flux-transformer. Below we explain in detail its design and fabrication.

The flux-transformer contact geometry is primarily used in high-T_c materials for transport studies of vortex correlation along the sample c axis. A set of conventional flux-transformer contact is similar to a set of four-probe contact in that it consists of four point contacts arranged in a row. The difference is that the two voltage contacts are placed at the opposite side of the sample. Measuring voltages at the opposite side of the sample from the applied current allows the observation of vortex correlation along the c axis. However, these conventional flux-transformer contacts, just as the conventional four-point contacts, render vortex studies vulnerable to the BL surface barrier effect. In order to study the c axis vortex correlation in BSCCO free from the BL surface barrier effect, it is necessary to adapt the flux-transformer pattern to Corbino-disk geometry. In our case, ideally the two voltage contacts should be placed on the bottom side of the sample within the ring. However, due to the opaque nature of the BSCCO material, photolithographic alignment of the bottom voltage contacts to the top Corbino-disk is nearly impossible. Hence we developed a unique method to place a pair of flux-transformer voltage contacts into our Corbino disk. We first etched holes into the sample (3 μm deep) using the Ar^+-ionmilling technique described in a previous publication.[8] Then gold was deposited simultaneously into the etched V_2 contacts, the surface V_1 contacts and the surface Corbino-disk ring contact. The ratio between the measured voltage V and the applied current I (note the current density is inevitably nonuniform for the Corbino disk contact geometry), V/I, is defined as the vortex resistance R. In these two sets of Corbino disk contacts, V_1 measures vortex dissipation R_1 at the BSCCO sample surface layers, and V_2 measures the vortex dissipation R_2 at layers 3 μm below the sample surface. Here for the purpose of comparison Comparison between R_1 and R_2 provides information on vortex correlation along the c axis without the BL surface barrier effect.

After the gold contact deposition, the BSCCO sample was then slightly overdoped (T_c=87 K) by annealing in air at 550 °C for 20 h. This annealing process also helps us to obtain the low contact resistances of less than 0.5 Ω per contact pair. We were able to measure the vortex solid dissipation with high precision because of this exceptionally low contact resistance. The sample was then placed in a superconducting solenoid with magnetic fields applied parallel to the c axis of the sample. The resistance was measured using a 16 Hz ac resistance bridge (linear resistance model LR-700) at a current value of 10 mA. The resistance bridge gives directly the resistance value R in reading.

We divide the discussion into two sections: we first discuss R_1 and R_2 independently in the first section, and then we compare R_1 and R_2 in the second section. We compare our Corbino-disk results in both sections to similar measurements using the conventional four-probe contact geometry. When an identical result is found in both the Corbino-disk and the conventional four-probe measurements, we infer that the measured vortex behavior is determined by the sample bulk vortex matter properties.

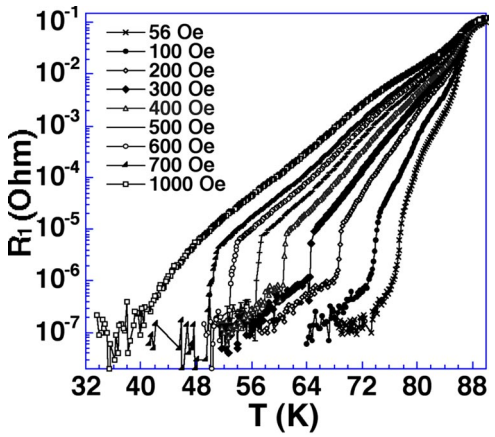

FIG. 2. R_1 vs T curves at magnetic fields ranging from 56 Oe to 1000 Oe. The sharp kinks represent the onset of the vortex lattice melting transition at temperature T_m. Below T_m the resistance decrease continues into the vortex solid phase.

We first discuss the surface vortex dissipation R_1. Figure 2 shows the resistance R_1 vs temperature curves at magnetic fields ranging from 56 Oe to 1000 Oe. With no exception, R_1 decreases with temperature at all fields and drops abruptly at the vortex melting temperature T_m seen at the kinks. These kinks are signatures of the vortex lattice melting transition. The kinks begin to smear at ~1000 Oe, indicating that the melting transition is approaching its critical end point. Our observed melting phase transition line (T_m vs H_a) and its critical end point agree with those measured in BSCCO using other experimental methods including conventional four-probe contacts.[9,10]

At temperatures below T_m and at a constant field, vortices are in the vortex solid phase. The vortex solid resistance can be clearly detected as shown in Fig. 2. These vortex solid dissipation data are among measurements of the highest precision.[4,5] We measured the activation energy of solid vortices U_0, which is the energy required to thermally activate vortices over energy barriers (bulk pinning barrier or surface barriers), by fitting the vortex solid resistance to an Arrhenius plot. Figure 3 plots the vortex solid resistance, R_1 vs $1/T$, for various applied fields H_a. The solid lines are the best fits to data in the Arrhenius form

$$\rho = \rho_0 \exp[-U_0/T], \tag{1}$$

where ρ_0 is the resistivity coefficient.[11] The activation energy U_0 is a function of H_a

$$U_0 \propto H_a - \alpha, \tag{2}$$

where α is a coefficient.

Below we compare our U_0 with that obtained using the four-probe contacts, where in fact U_0 may have been a measure of the BL surface barrier activation energy. The activation energies U_0 for different magnetic fields are extrapolated

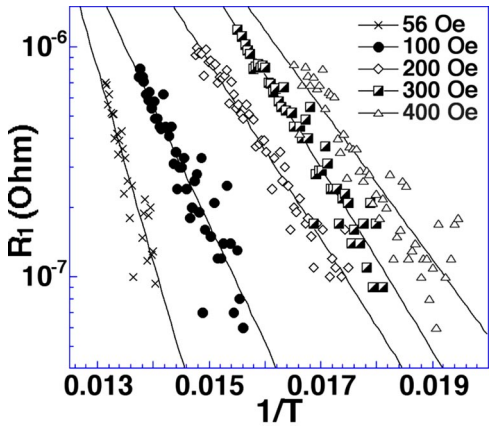

FIG. 3. Arrehnius plots, R_1 vs $1/T$, at magnetic fields of 56 Oe, 100 Oe, 200 Oe, 300 Oe, and 400 Oe. The solid lines are the best fits to the data.

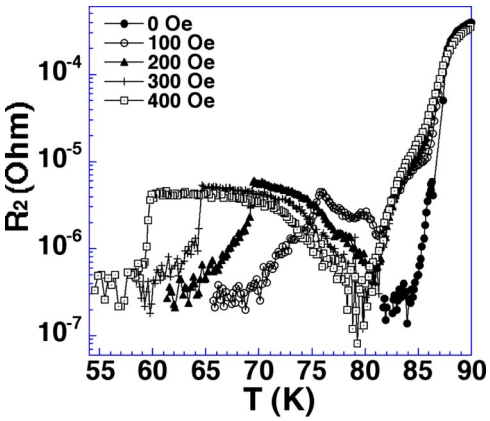

FIG. 5. R_2 vs T at various fields. The resistance first drops to the noise level at T_c and then gradually rises at lower temperatures, and finally drops abruptly again at T_m.

from the Arrhenius fittings of R_1 in Fig. 3 and plotted in Fig. 4. The solid line is the best fit to data as

$$U_0(K) = 10850H_a - 0.46. \tag{3}$$

Here 0.46 is the value for α in Eq. (2). The exponent α is equivalent to $\alpha \approx 1/2$ measured using the conventional four-probe contacts in BSCCO;[12] the prefactor of $U_0(K)$ is equivalent to that measured in Ref. 4. Thus U_0 is a measure of the bulk pinning activation energy, rather than the BL surface barrier activation energy. We have also measured the current dependence of the vortex solid resistance with current values ranging from 1 mA to 10 mA, and we observed non-Ohmic behavior, where the resistance increases with the current. This observation has also been reported in another Corbino-disk contact measurement.[2] Above studies indicate that the vortex lattice melting phase transition and the vortex solid state dissipation are determined by the sample bulk vortex properties.

We now discuss the pancake vortices resistance R_2. The resistance R_2 vs T curves are plotted in Fig. 5 for H_a ranging from 0 Oe to 400 Oe. At all fields, the resistance drops rapidly to the noise level ($10^{-7}\Omega$ at 10 mA) at T_c. At lower temperatures, the resistance rises to a plateau before it drops again at T_m. We interpret this resistance plateau as an incomplete sublimation of the 3D vortex solid to 2D pancakes,[13,14] where the pancakes at the deeper layers below the sample surface are still partially correlated with vortex pancakes at the surface layers. For if otherwise, when a vortex line dissociates completely into 2D pancakes, only the top layer pancakes should be mobile and the pancakes at 3 μm below the sample surface ($\approx$2000 layers of pancakes using the interlayer spacing of 16 Å) should be insensitive to the surface transport current. Again, our Corbino disk flux-transformer measurements as shown in Fig. 5 are identical to those measured using the conventional flux-transformer contact geometry.[15–17]

Finally, Fig. 6 compares the surface and hole resistances at 300 Oe. The melting onset temperatures and fields coincide and the resistances in the vortex solid phase are identical. The identical vortex solid resistances indicates that pancake vortices are correlated along the c axis. The applied current at the sample surface drives the whole vortex lines (at least to 3 μm below the sample surface) to circulate inside

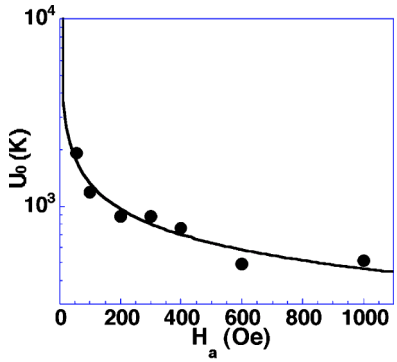

FIG. 4. Activation energy $U_0(K)$ vs H_a curve, where H_a is the applied magnetic field. The activation energy is extracted from the Arrehnius plot of R_1 for the vortex solid in Fig. 3.

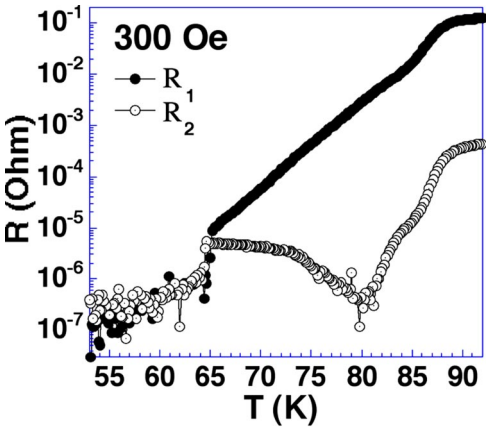

FIG. 6. Comparison of R_1 and R_2 at 300 Oe. Their melting transition onset temperatures and their resistances in the vortex solid phase coincide. The lower resistance value in R_2 between T_m and T_c indicates that the pancake vortices are not correlated at 3 μm below the sample surface in this temperature range.

the Corbino disk. Both resistances experience a dramatic decrease in value ($\Delta R_{T_c-T_m}$) from T_c to T_m, measuring 10^4 times for R_1 and 10^2 times for R_2. The resistance ratio R_1/R_2 is $\sim 10^3$ at T_c and drops to ~ 1 at T_m. These resistance drops and resistance ratios are identical to those measured using the conventional four-bar flux-transformer contacts.[17] If the BL surface barrier dominated the vortex liquid dissipation, then R_1/R_2 and $\Delta R_{1,T_c-T_m}$ and $\Delta R_{2,T_c-T_m}$ for the Corbino-disk flux-transformer contacts should differ from that for the conventional flux-transformer contacts, contrary to observation. If the pancakes were not fully correlated along the c axis in the vortex solid phase, then $R_{2,T<T_m}$ would be less than $R_{1,T<T_m}$. It thus can be inferred that the c-axis vortex correlation in BSCCO is determined by the sample bulk vortex matter properties.

The agreements found between above numerous Corbino-disk measurements with the conventional four-probe contact measurements indicate that we have measured true bulk vortex properties. These properties include vortex lattice melting transition, vortex solid and liquid dissipations and vortex correlation along the sample c axis. We thus conclude that, contrary to the BL surface barrier model,[1–3] it is the sample bulk vortex matter properties that determine the vortex transport properties in BSCCO.

This research was supported in part by NSF Grants DMR-9801738 and DMR-9501156, by the Director of the Office of Energy Research, Office of Basic Energy Sciences, Materials Sciences Division of the U.S. Department of Energy under Contract No. DEAC03-76SF00098.

*Current address: Department of Physics, Princeton University, Princeton, NJ 08544.

†Current address: Department of Physics and Center for Superconductivity Research, University of Maryland, College Park, MD 20742.

[1] D. T. Fuchs, E. Zeldov, M. Rappaport, T. Tamegai, S. Ooi, and H. Shtrikman, Nature (London) **391**, 373 (1998).

[2] D. T. Fuchs, R. A. Doyle, E. Zeldov, S. F. W. R. Rycroft, T. Tamegai, S. Ooi, M. L. Rappaport, and Y. Myasoedov, Phys. Rev. Lett. **81**, 3944 (1998).

[3] Y. Paltiel *et al.*, Phys. Rev. Lett. **85**, 3712 (2000).

[4] A. Mazilu, H. Safar, D. Lopez, W. K. Kwok, G. W. Crabtree, P. Guptasarma, and D. G. Hinks, Phys. Rev. B **58**, R8913 (1998).

[5] S. F. W. R. Rycroft, R. A. Doyle, D. T. Fuchs, E. Zeldov, R. J. Drost, P. H. Kes, T. Tamegai, S. Ooi, and D. T. Foord, Phys. Rev. B **60**, R757 (1999).

[6] J. Mirkovic, S. E. Savelev, E. Sugahara, and K. Kadowaki, Phys. Rev. Lett. **86**, 886 (2001).

[7] S. Ooi, T. Shibauchi, and T. Tamegai, Physica C **302**, 339 (1998).

[8] Y. M. Wang, A. Zettl, S. Ooi, and T. Tamegai, Phys. Rev. B **65**, 184506 (2002).

[9] R. Cubitt, E. M. Morgan, G. Yang, S. L. Lee, D. M. Paul, H. A. Mook, M. Yethiraj, P. H. Kes, T. W. Li, and A. A. Menovsky, Nature (London) **365**, 407 (1993).

[10] B. Khaykovich, E. Zeldov, D. Majer, T. W. Li, P. H. Kes, and M. Konczykowski, Phys. Rev. Lett. **76**, 2555 (1996).

[11] The resistivity coefficient ρ_0 is also a function of temperature and magnetic field. However, at our vortex solid phase where $T < 0.5T_c$, the temperature dependence of ρ_0 is almost constant (Ref. 12). Therefore, we may only concern ourselves with ρ_0's dependence on the magnetic field.

[12] T. T. M. Palstra, B. Batlogg, R. B. van Dover, L. F. Schneemeyer, and J. V. Waszczak, Phys. Rev. B **41**, 6621 (1990).

[13] X. G. Qiu, V. V. Moshchalkov, and J. Karpinski, Phys. Rev. B **62**, 4119 (2000).

[14] T. Blasius, C. Niedermayer, J. L. Tallon, D. M. Pooke, A. Golnik, and C. Bernhard, Phys. Rev. Lett. **82**, 4926 (1999).

[15] D. Lopez, E. F. Righi, G. Nieva, and F. de la Cruz, Phys. Rev. Lett. **76**, 4034 (1996).

[16] C. D. Keener, M. L. Trawick, S. M. Ammirata, S. E. Hebboul, and J. C. Garland, Phys. Rev. Lett. **78**, 1118 (1997).

[17] D. T. Fuchs, R. A. Doyle, E. Zeldov, D. Majer, W. S. Seow, R. J. Drost, T. Tamegai, S. Ooi, M. Konczykowski, and P. H. Kes, Phys. Rev. B **55**, R6156 (1997).